AD-A064 747 DREXEL UNIV PHILADELPHIA PA DEPT OF MATERIALS ENGINEERING F/G 11/4
STRUCTURE, STABILITY AND TOUGHNESS OF (CO,CR)-(CR,CO) 7C3.(U)
NOV 78 L Y LIN, M H ABDELLATIF, A LAWLEY N00014-76-C-0205

UNCLASSIFIED NL

| OF |
AD
AD 64747

END
DATE FILMED
4-79
DDC

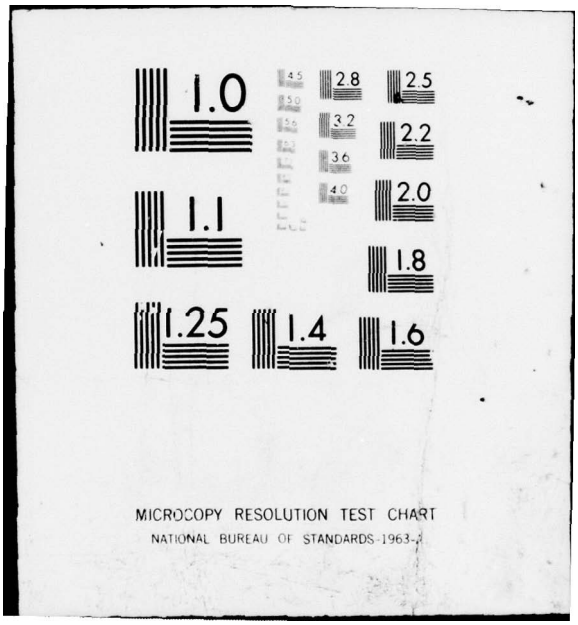
1.0
1.1
1.25
1.4
1.6
1.8
2.0
2.2
2.5
2.8
3.2
3.6
4.0
4.5
5.0
5.6
MICROCOPY RESOLUTION TEST CHART
NATIONAL BUREAU OF STANDARDS-1963-A

LEVEL II

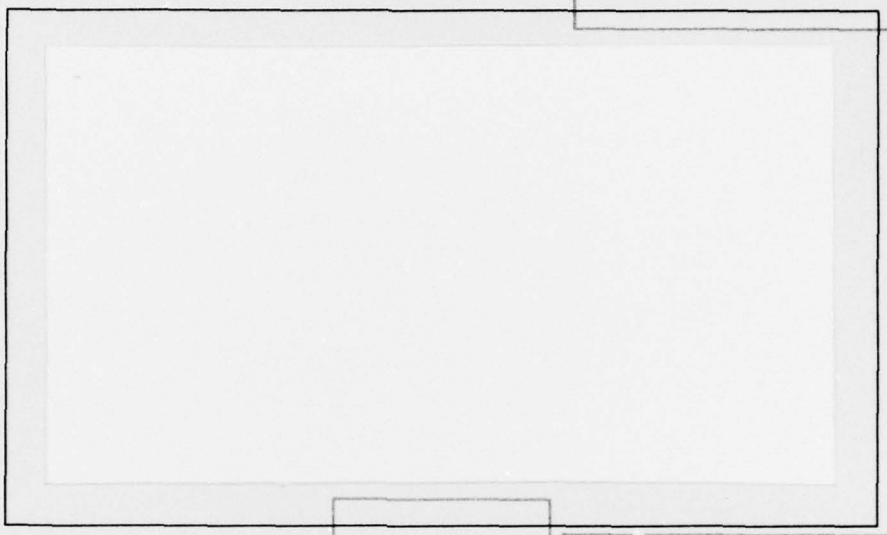

Drexel University

(12)

LEVEL II

STRUCTURE, STABILITY AND TOUGHNESS OF (Co,Cr)-$(Cr,Co)_7C_3$

(10) L. Y. Lin, M. H. AbdelLatif and A. Lawley

(11) November 1978

(12) 21 p.

(9) Technical Report
Office of Naval Research
Arlington, Virginia 22217

(15) Contract #N00014-76-C-0205

Drexel University
Department of Materials Engineering
Philadelphia, Pennsylvania 19104

ABSTRACT

The effect of thermal treatment on the toughness of fibrous Co,Cr-$(Cr,Co)_7C_3$ in-situ composites has been examined. Several regimes of thermal cycling were imposed with a T_{max} of 1121°C and also isothermal exposure at 1121°C ($0.89T_M$). Toughness was evaluated by the work of fracture test in terms of the energy of fracture G_f and peak load P_ℓ. Response confirms excellent long-term stability and property integrity to the cyclic and fixed temperature exposures. Some of the treatments actually enhance toughness by a factor of about two over that of the as-grown material. Fibers break by cleavage and the matrix shears to link up fiber breaks. The absence of fiber pull-out or interface delamination confirms the strength of the matrix-fiber interface bond. Splitting of fibers along their length provides a mechanism for energy absorption with an associated increase in the work of fracture. A tentative explanation for the changes in G_f and P_ℓ with thermal treatment is given; this involves the interplay of residual stress, stress relaxation and fiber degradation.

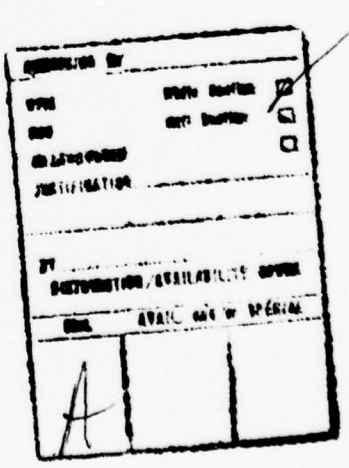

Introduction

The substantial increase in efficiency of a gas turbine engine with increased inlet temperatures has led to the consideration of metal matrix composites for use as the blade material. In particular, in-situ composites, grown by directional solidification, consisting of high-strength fibers or plates in a ductile and tough matrix provide outstanding high temperature properties. This class of materials represents a major innovation in gas turbine technology for applications in aerospace, shipboard, and on land.

Intrinsically, in-situ composites are stable at elevated temperatures, a characteristic derived from their solidification under near equilibrium conditions, coupled with the formation of low-energy interface boundaries. However, microstructural instability and attendant property degradation may occur as a result of prolonged high-temperature exposure, thermal cycling, or the presence of a thermal gradient. Since these reflect normal service conditions, it is necessary to assess composite integrity.

While it is recognized that toughness is a critical design parameter, the data base re impact loading is limited (1,2). Similarly few attempts have been made to interpret toughness in terms of microstructure (1,2). In the present study, the objective has been to examine the work of fracture in the Co,Cr-$(Cr,Co)_7C_3$ fibrous composite (V_f = 0.3) as a function of isothermal and thermal cycling excursions. The nature of the constituents, the high temperature strength and the melting point suggest the viability of this system for elevated temperature applications.

The work of fracture in as-grown Co,Cr-$(Cr,Co)_7C_3$ has been found to be dependent on fiber orientation and can reach a level about three times that of cast MarM-302, (3). Fiber diameter also affected work of fracture in this system; toughness decreased as fiber diameter decreased (3). A minimum

in toughness has been reported between 400°C and 950°C (4). Recently, promising improvements in the toughness of this composite system have been observed at temperatures below 1000°C by alloying with nickel. It is argued that the nickel increases the ductility of the matrix, perhaps through an increase in the stacking fault energy (5). No studies have been reported on the effect of isothermal elevated temperature exposure or thermal cycling on toughness in Co,Cr-$(Cr,Co)_7C_3$. Isothermal treatments can give rise to coarsening and spheroidization of the composite microstructure, i.e., physicochemical instability. With thermal cycling the thermal expansion mismatch, mutual solubility and phase stability of the co-existing constituents are of primary importance.

Experimental Procedure

A. Composite Preparation

Master alloy rods were prepared from 99.99% purity cobalt and chromium and spectographic grade carbon by induction melting in an alumina crucible under argon and casting in a stainless steel mold. The rods were then placed in a 9.525mm dia. alumina tube and directionally solidified at 7×10^{-6}m/s in an induction furnace under argon. The temperature gradient at the liquid-solid interface was in excess of 25×10^{3}°C/m which gave a G/R value > 36×10^{8}°C.s/m^2.

B. Thermal Treatments

Three thermal cycling regimes were selected: 80°C to 1121°C, 400°C to 1121°C and 538°C to 1121°C. The melting point of the monovariant eutectic is 1300°C (6) so the T_{max} of 1121°C corresponds to a homologous temperature of 0.89. Various levels of T_{min} were used in order to evaluate the effect of cyclic temperature interval ΔT ($=T_{max} - T_{min}$) on the work of fracture. As a further mode of thermal treatment, a group of specimens was cycled between 400°C and 1121°C but with a superimposed hold time of 3600s at T_{max}

during each cycle. Each of the four regimes involved up to 3000 cycles. Isothermal exposures were also performed at 1121°C (i.e. at the same temperature as T_{max} in thermal cycling) for times up to 252 x 10^4s.

Specimens approximately 28.5mm in length were cut from the center portion of the directionally solidified ingots using a diamond slitting wheel. For isothermal annealing these were then sealed in quartz tubes under argon. The thermal cycling facility consisted of a quartz lamp radiant heat reflector furnace (having a heating zone 254mm in length) coupled with a data track programmer and temperature controller. With this arrangement the required values of T_{max} and T_{min} (±2°C) could be preset. The specimen was placed in a quartz tube under flowing argon and the tube located along the focal axis of the reflector furnace. Cycle frequency was relatively high; typical cycle times, i.e. T_{min} to T_{max} to T_{min} were 420s and 270s for the 400°C to 1121°C and 538°C to 1121°C excursions, respectively.

C. Work of Fracture Determination

To determine the work of fracture, the technique and specimen configuration developed by Tattersall and Tappin (7) was used. Specimens, illustrated in Figure 1, were of square cross-section (6.35mm x 6.35mm) and 28.5mm in length, with a ligament at the center in the shape of an isosceles triangle; ligament width (t) was 0.76mm. Specimens were loaded to failure under three-point loading in the frame of a standard Instron testing machine. In this form of test only a small load is required to initiate crack growth and the relatively slow rate of loading mitigates against energy loss due to the vibration and kinetic energy characteristic of the standard Charpy test. A cross-head speed of 8 x 10^{-4}mm/s was imposed on the three-point loading fixture.

Work of fracture specimens in the as-grown condition and after thermal treatment were precision ground to give the square cross-section. The ligament in the center was made with a 0.76mm wide diamond wheel. All specimens were

oriented such that the carbide fiber reinforcement ran perpendicular to the plane of the triangular ligament section. The form of the load-deflection trace is shown schematically in Figure 1. Average values of the work of fracture (J/m^2) were determined as the ratio of the area under the load-deflection curve to the nominal area of the triangular ligament.

D. Metallography

Metallographic sections were prepared parallel and normal to the fiber direction for optical microscopy. Some specimens were deep-etched in aqua regia and examined in the scanning electron microscope to reveal morphological and surface changes in the carbide fibers as a result of isothermal exposure or thermal cycling. Fracture surfaces from the work of fracture specimens were examined directly by scanning electron microscopy.

Results and Discussion

A. As-Grown Composites

Optical micrographs of the as-grown composites are illustrated in Figures 2(a) and 2(b) for the transverse and longitudinal orientations, respectively. Consistent with previous observations on this system by Thompson and Lemkey (6), the aligned fibrous carbide reinforcement is highly irregular in terms of cross-sectional dimensions and geometry. Extensive branching of the carbide is evident and aspect-ratio varies over a wide range. Similarly the inter carbide spacing varies about a mean of $\sim$4μm. This is again comparable to the scale of the microstructrure reported by Thompson and Lemkey for similar growth rates (6). Faceting of fiber cross-sections is evident in transverse microstructures (Figure 2(a)) and is further illustrated by scanning electron microscopy, Figure 2(c). In the latter micrograph, the matrix has been etched away to reveal fiber morphology and

surface condition. Fiber surfaces in the as-grown composite are relatively smooth. Faceting reflects hexagonal symmetry of the carbide reinforcement.

The average work of fracture level G_f in the as-grown condition is 14.7 kJ/m^2 with an associated peak load P_ℓ of 2669 N. These values are in good agreement with those reported by Thompson (3) for composites of the same fiber orientation grown at 8×10^{-6} m/s.

On a relative scale, the Co,Cr-$(Cr,Co)_7C_3$ composites exhibit a combination of low toughness and high fracture stress. This mandates a 'hard' load cell in carrying out the work of fracture test in order to prevent uncontrolled crack propagation with associated kinetic energy loss in the fracture pieces. The 'tail' on the right-hand load-deflection curve in Figure 1 reflects increased toughness (8). Fracture begins at the peak load P_ℓ; the instantaneous load drop corresponds to the catastrophic part of the crack growth while the 'tail' reflects the controlled part. While the extent of the 'tail' area varied from specimen to specimen, it was typcially in the range 5-10% of the total area under the load-displacement curve.

B. Thermally Treated Composites

The effect of the three thermal cycling regimes on work of fracture G_f and peak load P_ℓ is shown in Figures 3, 4 and 5, and for the superimposed hold time at T_{max} in Figure 6. The corresponding dependence of G_f and P_ℓ on isothermal exposure is given in Figure 7. The extent of the 'tail' area was similar to that in the as-grown condition; no significant differences could be established between the various thermal treatments and the extent of the 'tail' area.

Considering all the thermal cycling treatments imposed, it is clear that the general pattern is for G_f and P_ℓ to increase and reach peak values after a relatively small number of cycles (150-600). Further cycling then leads to

a decrease in both parameters. Such an increase in both G_f and P_ℓ reflects an enhancement of the mechanical properties. However, the increase in G_f is the more significant of the two; thus, G_f reaches a value about twice that for the material in the directionally solidified condition. It is also interesting to observe that while G_f peaks and then decreases, the level of G_f after 3000 cycles is still at or close to that of the as-grown material. The worst condition in terms of the level of G_f occurs for the thermal cycling treatment with the maximum ΔT, i.e., 80°C to 1121°C, Figure 3. Here there is a decrease ~25% in G_f after 2500 cycles.

The initial increase in G_f and P_ℓ on thermal cycling is attributed to axial thermal mismatch stresses caused by the difference in thermal expansion coefficients of the two constituents in the composite (9-11). These stresses have been calculated for each of the thermal cycling programs used (12); they reach a maximum at T_{min} and a minimum at T_{max}. Such stresses could lead to cyclic thermal fatigue hardening. The magnitude of these thermal residual stresses is proportional to ΔT. It is therefore expected that their effect on G_f and P_ℓ (measured in terms of peak values) will be more pronounced in the thermal cycling regime having the largest ($T_{max} - T_{min}$) difference. This is, in fact, the case as seen by a comparison of Figures 3, 4 and 5; the 80°C to 1121°C excursions maximize the increases in G_F and P_ℓ, Figure 3.

Subsequent decreases in G_f and P_ℓ may be explained on the basis of relaxation of the thermal stresses, either by matrix creep or dynamic recovery. A further factor could be fiber degradation during thermal cycling. There is no apparent fiber degradation after 3000 cycles between 538°C and 1121°C, Figure 8(a). However, some degradation, as reflected in fiber surface appearance, is noted after 3057 cycles between 400°C and 1121°C, Figure 8(b).

The variation of G_f and P_ℓ with cyclic treatment involving a superimposed hold time is similar to that described above, Figure 6. Increases in G_f and P_ℓ with cycling are less pronounced as compared to thermal cycling with no hold time. With a hold time imposed at T_{max} there will be a longer time available for matrix creep, dynamic recovery or fiber degradation; individually or in combination, these could give rise to a lower increment in G_f or P_ℓ on thermal cycling compared to the increment resulting from thermal cycling without hold time.

Both G_f and P_ℓ increase with isothermal treatment at 1121°C, Figure 7. Work of fracture G_f reaches a maximum after about five days ($\sim 4 \times 10^5$s) then decreases slightly but to a level higher than that of G_f in the as-grown condition. Peak load P_ℓ increases over the same time scale and then remains constant. This confirms the excellent high-temperature stability of this composite at a homologous temperature of 0.89. Microstructurally, after isothermal exposure, fibers look similar to those in the as-grown composite. An example is shown of fibers after 18×10^5s at 1121°C in Figure 8(c). There is no evidence of surface degradation or serrations. Further studies are needed to arrive at a deeper understanding of the transient increases in G_f and P_ℓ in terms of microstructural change(s) brought about by isothermal exposure and/or thermal cycling.

On a macroscopic scale, the fracture surfaces of thermally cycled and isothermally treated composites are relatively flat indicative of brittle fracture. Microscopically, the fibers fail in a brittle mode accompanied by ductile fracture of the matrix. The matrix shears to link the fiber (cleavage) breaks, Figure 9(a). There was no evidence for fiber pull-out or delamination at fiber matrix interfaces. Thus, these are not operative sources of energy absorption as the crack propagates through the ligament. The absence of delamination is a characteristic of in-situ composites and

reflects integrity of the low energy interface between matrix and reinforcement (1). Some occasional fiber splitting in the longitudinal direction of the fibers was observed. Figure 9(b) shows this phenomenon after thermal cycling between 400°C and 1121°C. This has the beneficial effect of diverting a propagating crack, thereby enhancing toughness. Thompson (3) has suggested that the splitting may be caused by the stress generated at the boundary between the plastic and elastic zone at the tip of the crack propagating in the matrix.

Conclusions

For the conditions of thermal cycling and isothermal exposure examined, the directionally solidified Co,Cr-$(Cr,Co)_7C_3$ composite shows excellent stability, as measured by the work of fracture and peak load. Some of the thermal treatments actually enhance toughness - to the extent that there is a two-fold increase in the work of fracture over that of the directionally solidified condition.

Fractography confirms a brittle fracture mode with cleavage of fibers and matrix shearing to link up fiber breaks. The absence of fiber pull-out or interface delamination confirms interface bond integrity. Occasional splitting of fibers along the length causes crack diversion and is a source of enhanced toughness.

References

1. Lawley, A., Conference on In-Situ Composites-II, Edited by M. R. Jackson, J. L. Walter, F. D. Lemkey and R. W. Hertzberg, Xerox Individualized Publishing, Lexington, Mass., p. 451, 1976.

2. Stoloff, N. S. in Advances in Composite Materials, Edited by G. Piatti, Applied Science Publishers Ltd., London, p. 274, 1978.

3. Thompson, E. R., J. Composite Materials, Vol. 5, p. 235, 1971.

4. Sahm, P. R. and Varga, T., Proc. Conference on In-Situ Composites, National Materials Advisory Board, Report #NMAB 308-II, National Academy of Sciences - National Academy of Engineering, Washington, D. C., p. 239, 1973.

5. Nicoll, A. R. and Sahm, P. R., Proc. Int. Conference on Composite Materials, AIME, New York, Vol. 2, p. 904, 1976.

6. Thompson, E. R. and Lemkey, F. D., Met. Trans., Vol. 1, p. 2799, 1970.

7. Tattersall, H. G. and Tappin, G., Journal of Materials Science, Vol. 1, p. 296, 1966.

8. Yue, A. S. and Kaba, B. T., in Composite Reliability, ASTM STP #580, American Society for Testing and Materials, Phila., Pa., p. 504, 1975.

9. Woodford, D. A., J. Materials Science and Engineering, Vol. 24, p. 257, 1976.

10. Gell, M., AGARD Conference Proc. #156, "Directionally Solidified In-Situ Composites", Editors: E. R. Thompson and P. R. Sahm, Technical Editing and Reproduction Ltd., London, p. 117, 1974.

11. Breinan, E. M., Thompson, E. R. and Lemkey, F. D., see reference #4, p. 201.

12. AbdelLatif, M. H. and Lawley, A., unpublished work.

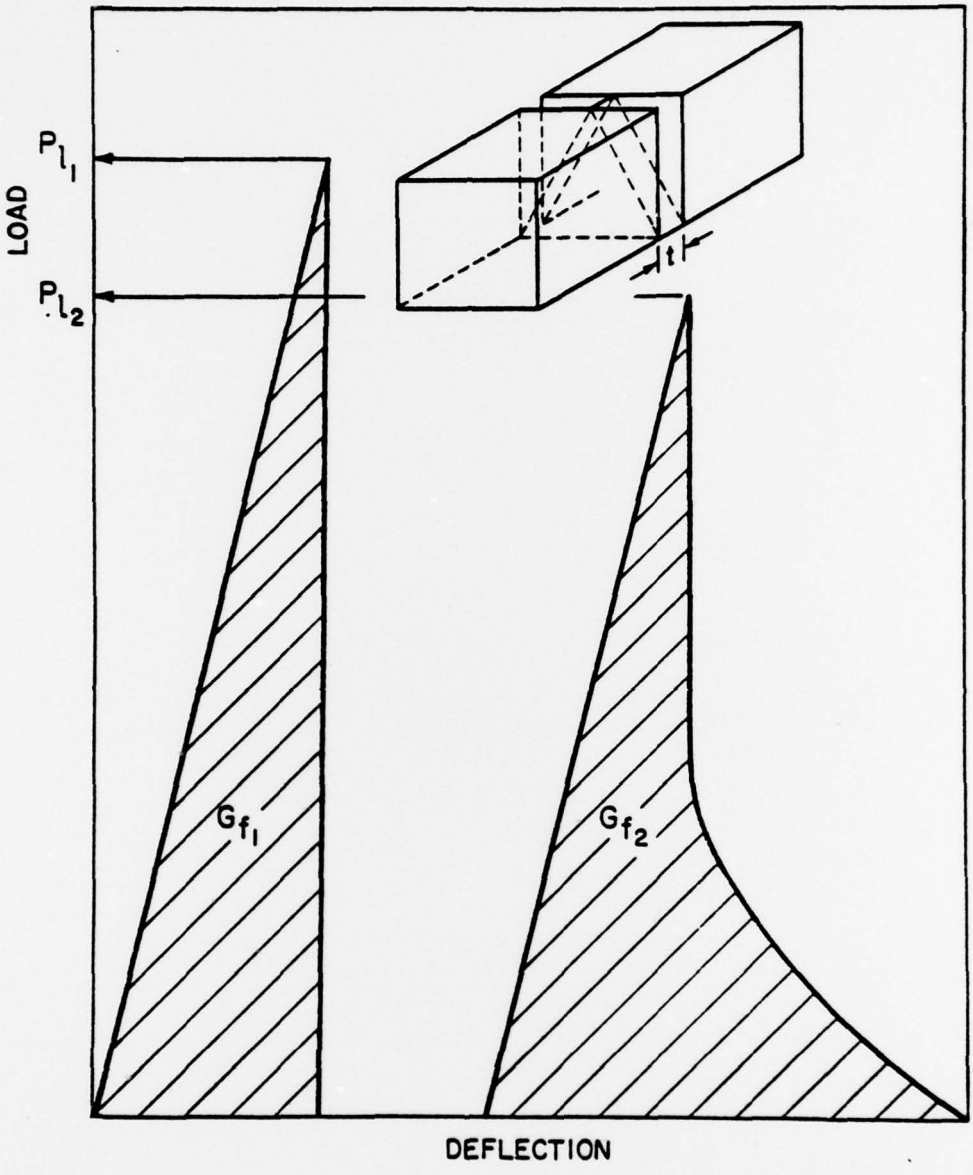

Figure 1. The work of fracture specimen geometry and schematic load-deflection traces.

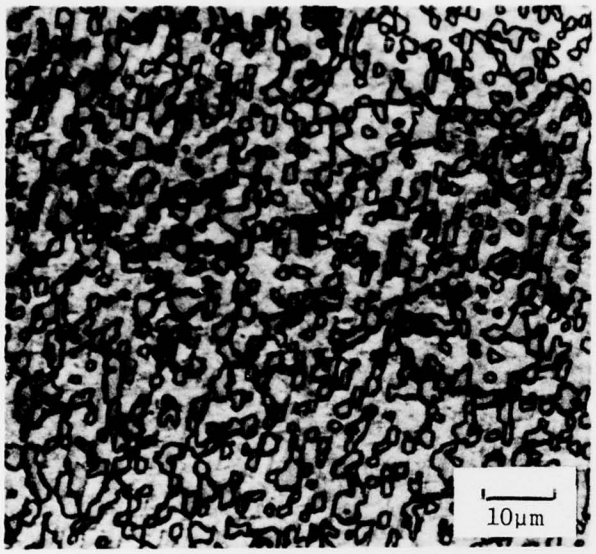

(a)

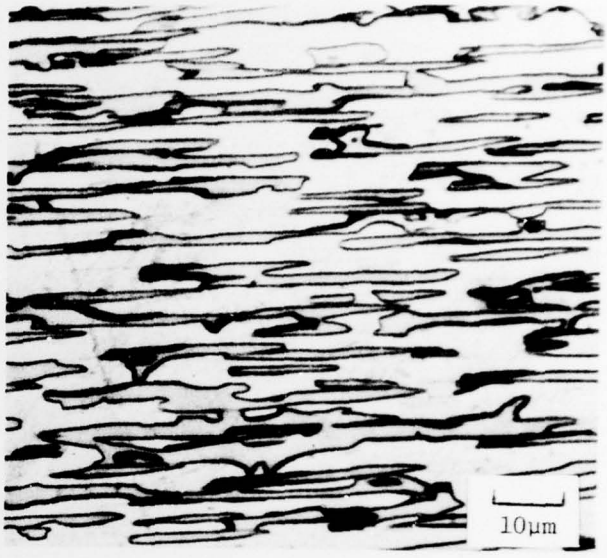

(b)

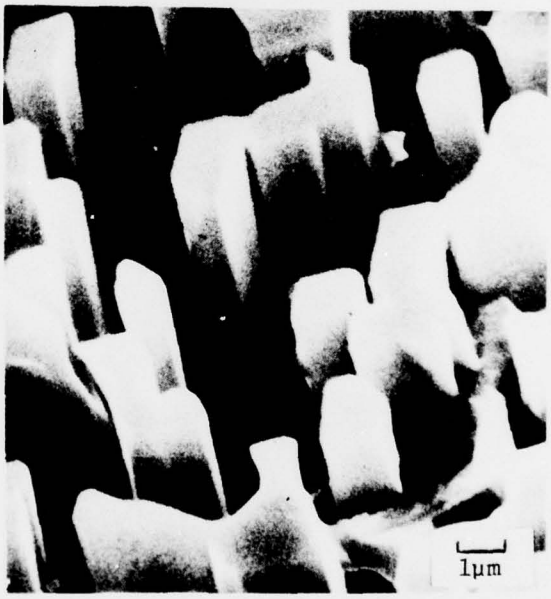

(c)

Figure 2. Microstructure of the as-grown composite: a) transverse; b) longitudinal sections; c) fiber morphology (SEM).

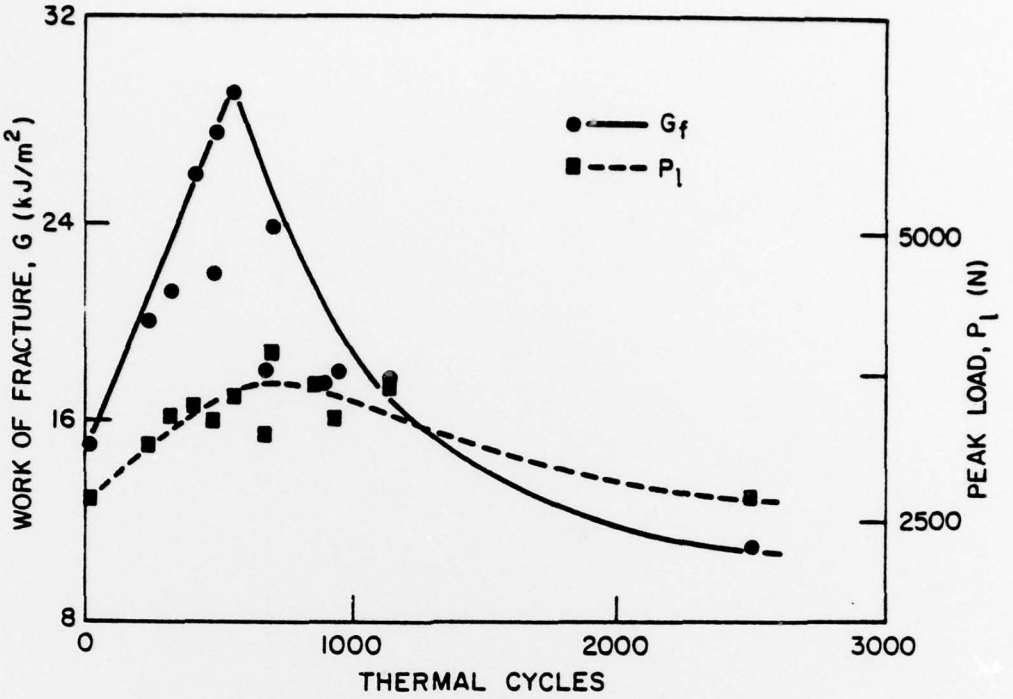

Figure 3. Work of fracture (G_f) and peak load (P_ℓ) as a function of thermal cycling between 80°C and 1121°C.

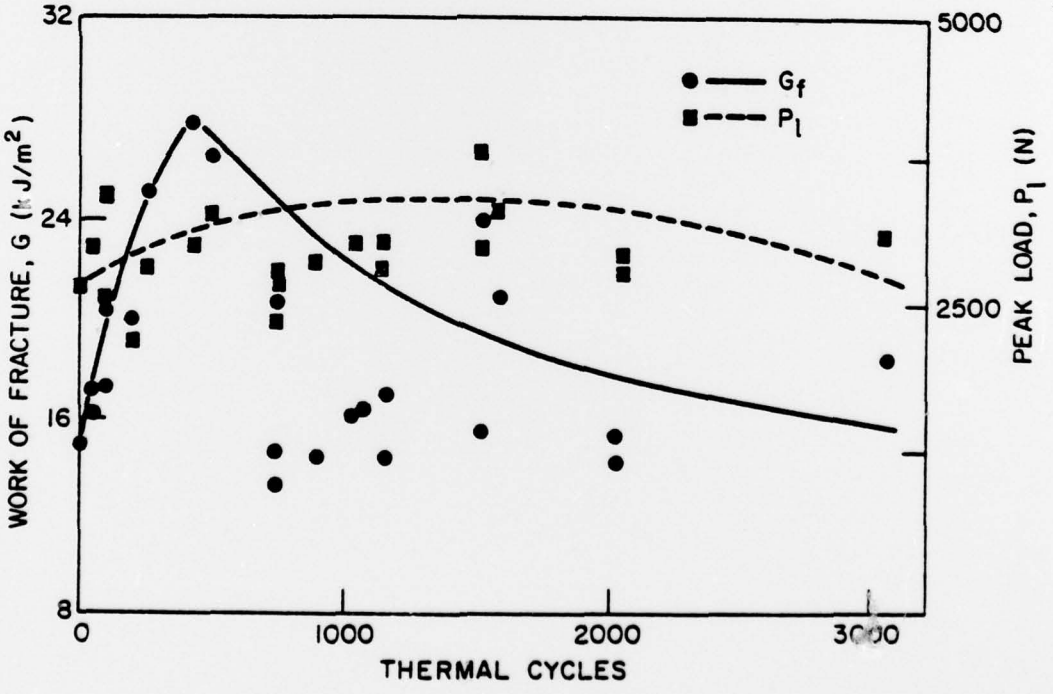

Figure 4. Work of fracture (G_f) and peak load (P_ℓ) as a function of thermal cycling between 400°C and 1121°C.

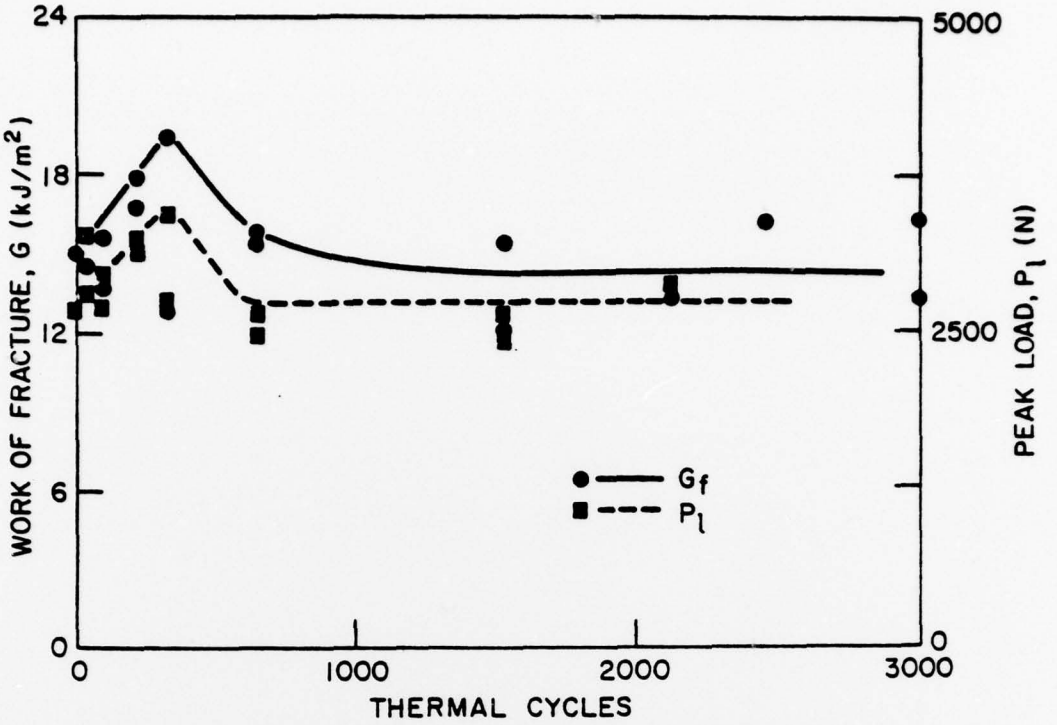

Figure 5. Work of fracture (G_f) and peak load (P_ℓ) as a function of thermal cycling between 538°C and 1121°C.

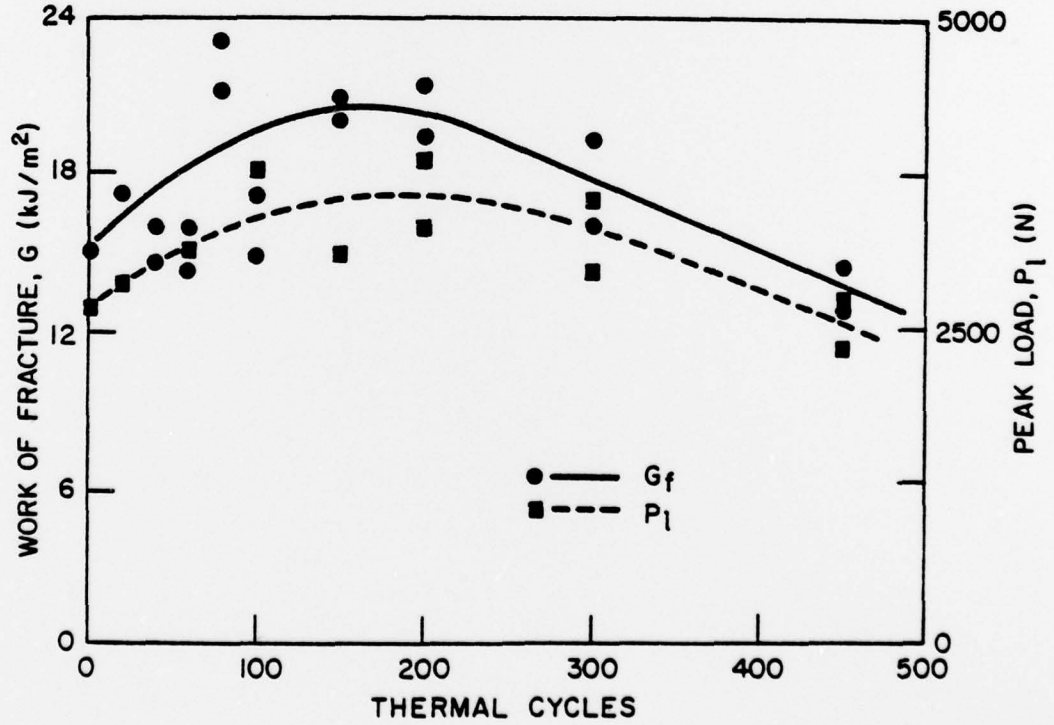

Figure 6. Work of fracture (G_f) and peak load (P_ℓ) as a function of thermal cycling (400°C to 1121°C) with a hold time of 3600s at T_{max}.

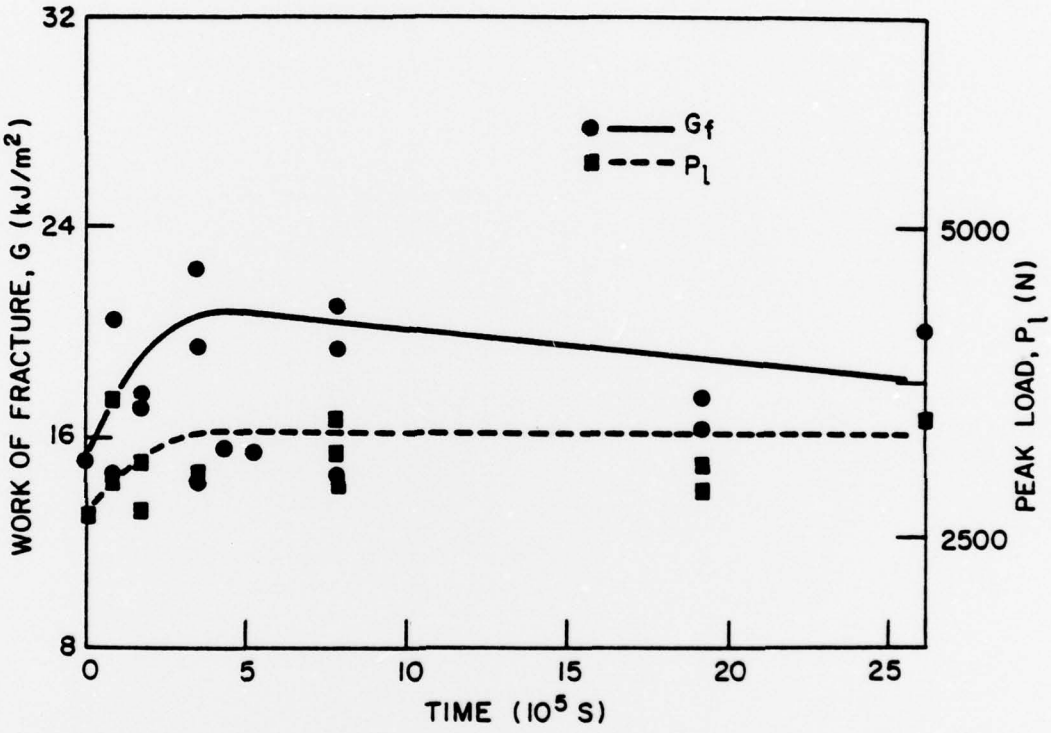

Figure 7. Work of fracture (G_f) and peak load (P_l) as a function of isothermal treatment at 1121°C.

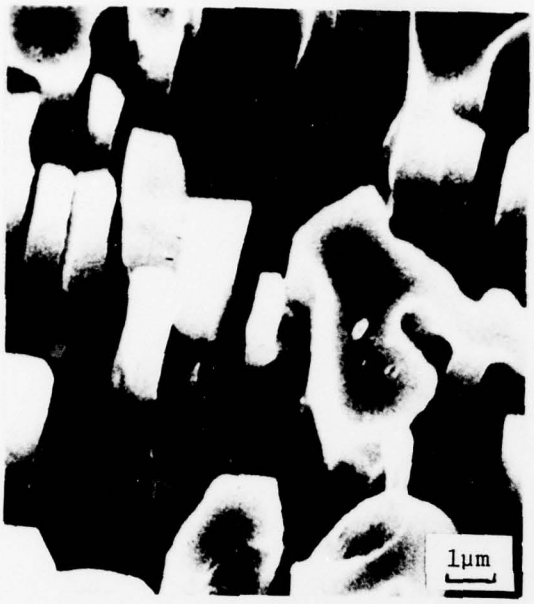

(a)

(b)

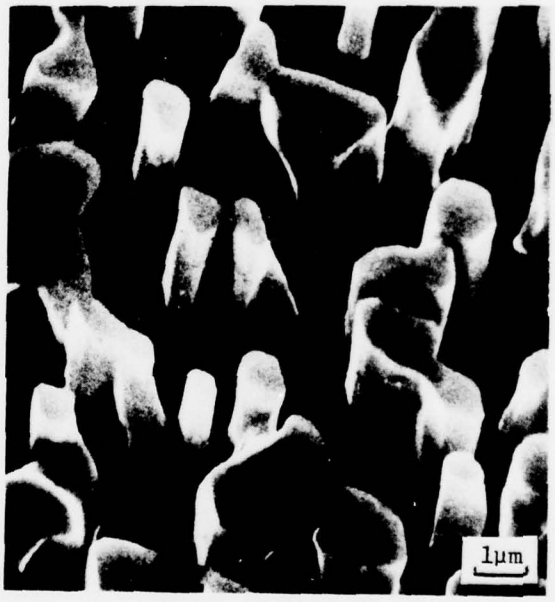

(c)

Figure 8. Scanning electron micrographs of thermally treated composites after deep-etching to reveal fiber morphology:
(a) 3000 cycles between 538°C and 1121°C
(b) 3057 cycles between 400°C and 1121°C
(c) 180 x 10^4s at 1121°C.

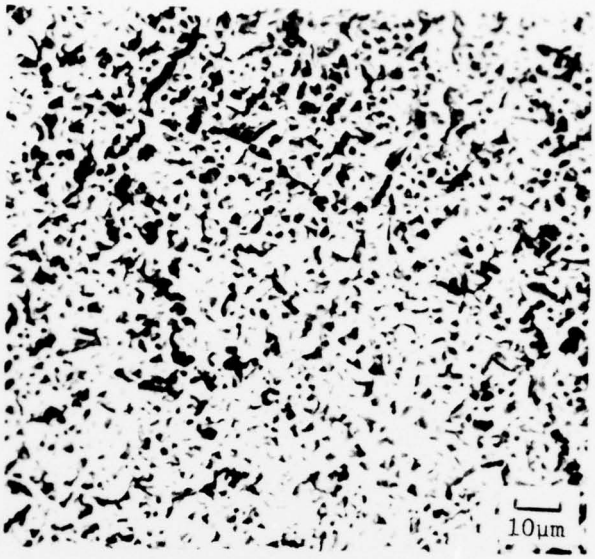

(a)

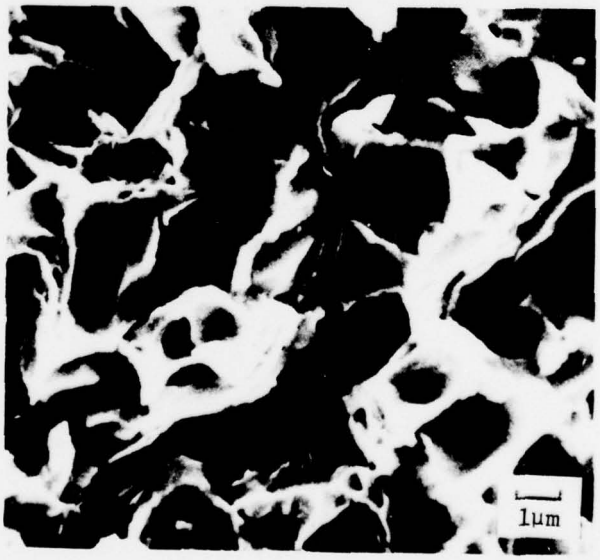

(b)

Figure 9. Scanning electron micrographs of fracture surfaces of a thermally cycled composite: 431 cycles between 400°C and 1121°C.

Unclassified

SECURITY CLASSIFICATION OF THIS PAGE (When Data Entered)

REPORT DOCUMENTATION PAGE		READ INSTRUCTIONS BEFORE COMPLETING FORM
1. REPORT NUMBER: 1	2. GOVT ACCESSION NO.	3. RECIPIENT'S CATALOG NUMBER
4. TITLE (and Subtitle): Structure, Stability and Toughness of (Co,Cr)-$(Cr,Co)_7C_3$		5. TYPE OF REPORT & PERIOD COVERED: Technical Report, November 1978 6. PERFORMING ORG. REPORT NUMBER
7. AUTHOR(s): L. Y. Lin, M. H. AbdelLatif and A. Lawley		8. CONTRACT OR GRANT NUMBER(s): N00014-76-C-0205
9. PERFORMING ORGANIZATION NAME AND ADDRESS: Drexel University, Dept. of Materials Eng. Philadelphia, Pa. 19104		10. PROGRAM ELEMENT, PROJECT, TASK AREA & WORK UNIT NUMBERS
11. CONTROLLING OFFICE NAME AND ADDRESS: Office of Naval Research Arlington, Va. 22217		12. REPORT DATE: November 1978 13. NUMBER OF PAGES: 16
14. MONITORING AGENCY NAME & ADDRESS(if different from Controlling Office)		15. SECURITY CLASS. (of this report) 15a. DECLASSIFICATION/DOWNGRADING SCHEDULE

16. DISTRIBUTION STATEMENT (of this Report)

Unlimited

17. DISTRIBUTION STATEMENT (of the abstract entered in Block 20, if different from Report)

18. SUPPLEMENTARY NOTES

19. KEY WORDS (Continue on reverse side if necessary and identify by block number)

metal matrix composites, directional solidification, isothermal and thermal cycling, work of fracture, microstructure

20. ABSTRACT (Continue on reverse side if necessary and identify by block number)

The effect of thermal treatment on the toughness of fibrous Co,Cr-$(Cr,Co)_7C_3$ in-situ composites has been examined. Several regimes of thermal cycling were imposed with a T_{max} of 1121°C and also isothermal exposure at 1121°C (0.89 T_M). Toughness was evaluated by the work of fracture test in terms of the energy of fracture G_f and peak load P_ℓ. Response confirms excellent long-term stability and property integrity to the cyclic and fixed temperature exposures. Some of the treatments actually enhance toughness by a factor of

DD FORM 1 JAN 73 1473 EDITION OF 1 NOV 65 IS OBSOLETE
S/N 0102-014-6601

Unclassified

SECURITY CLASSIFICATION OF THIS PAGE (When Data Entered)

20. (Continued)

about two over that of the as-grown material. Fibers break by cleavage and the matrix shears to link up fiber breaks. The absence of fiber pull-out or interface delamination confirms the strength of the matrix-fiber interface bond. Splitting of fibers along their length provides a mechanism for energy absorption with an associated increase in the work of fracture. A tentative explanation for the changes in G_f and P_ℓ with thermal treatment is given; this involves the interplay of residual stress, stress relaxation and fiber degradation.